



“Authors may post the original unedited, unformatted, peerreviewed versions of their articles on their university or company websites at no charge”  
[https://apsjournals.apsnet.org/pb-assets/Intellectual\\_Property-1550840912083.pdf](https://apsjournals.apsnet.org/pb-assets/Intellectual_Property-1550840912083.pdf)

This document is the original unedited, unformatted, peerreviewed version of an article published in Plant Disease, copyright © The American Phytopathological Society (APS). To access the final edited and published work see <http://doi.org/10.1094/PDIS-08-23-1540-RE>

**Full citation reference:**

Pons-Solé, Gemma, Laura Torguet, Neus Marimon, Xavier Miarnau, Elena Lázaro, Antonio Vicent Civera, and Jordi Luque. “Modeling the Airborne Inoculum of *Polystigma Amygdalinum* to Optimize Fungicide Programs against Almond Red Leaf Blotch.” *Plant Disease*, September 27, 2023. <https://doi.org/10.1094/pdis-08-23-1540-re> .

**Document downloaded from:**



1 **Modeling the airborne inoculum of *Polystigma amygdalinum* to optimize**  
2 **fungicide programs against almond red leaf blotch**

3

4 Gemma Pons-Solé<sup>1,2</sup>, Laura Torguet<sup>3</sup>, Neus Marimon<sup>3</sup>, Xavier Miarnau<sup>3</sup>, Elena Lázaro<sup>4</sup>,  
5 Antonio Vicent<sup>4</sup>, and Jordi Luque<sup>1\*</sup>

6

7 <sup>1</sup>*Sustainable Plant Protection, Institut de Recerca i Tecnologia Agroalimentàries (IRTA)*  
8 *Cabrils, Ctra. de Cabrils km 2, E-08348 Cabrils, Spain*

9 <sup>2</sup>*Plant Physiology Laboratory, Universitat Autònoma de Barcelona (UAB), 08193*  
10 *Bellaterra, Spain*

11 <sup>3</sup>*Fruit Production Program, Institut de Recerca i Tecnologia Agroalimentàries (IRTA)*  
12 *Fruitcentre, PCiTAL, Park of Gardeny, Fruitcentre Building, E-25003 Lleida, Spain*

13 <sup>4</sup>*Centre de Protecció Vegetal i Biotecnologia, Institut Valencià d'Investigacions Agràries*  
14 *(IVIA), Ctra. CV-315 km 10.7, 46113 Moncada, Spain*

15 \*Corresponding author: Jordi Luque; E-mail: jordi.luque@irta.cat

16

17 **Keywords:** decision support system, disease control, epidemiology, modeling,  
18 *Polystigma amygdalinum*, *Prunus dulcis*, red leaf blotch

19

20 **Funding:** Instituto Nacional de Investigación y Tecnología Agraria y Alimentaria (INIA,  
21 Spain); Grant Number: RTA2017-00009-C04-01, and Agencia Estatal de Investigación  
22 (AEI, Spain); Grant Number: PID2020-114648RR-C31  
23 (MCIN/AEI/10.13039/501100011033). G.P.-S. is supported by a predoctoral grant from  
24 AEI; Grant Number: PRE2018-085207. J.L., L.T., and X.M. are supported by the  
25 CERCA Program, Generalitat de Catalunya.

26 **ABSTRACT**

27 Red leaf blotch (RLB) of almond, caused by the ascomycete *Polystigma*  
28 *amygdalinum*, is a severe foliar disease endemic in the Mediterranean Basin  
29 and Middle East. Airborne ascospores of *P. amygdalinum* were monitored from  
30 2019 to 2021 in two almond orchards in Lleida, Spain, and a Bayesian beta  
31 regression was used to model its seasonal dynamics. The selected model  
32 incorporated accumulated degree-days (ADD) and ADD considering both vapor  
33 pressure deficit and rainfall as fixed effects, and a random effect for the year  
34 and location. The performance of the model was evaluated in 2022 to optimize  
35 RLB fungicide programs, by comparing the use of model predictions and action  
36 thresholds with the standard program. Two variants were additionally  
37 considered in each program to set the frequency between applications, based  
38 on: i) a fixed frequency of 21 days, or ii) specific meteorological criteria  
39 (spraying within seven days after rainfalls greater than 10 mm, with daily mean  
40 temperatures between 10 and 20°C, and with minimum 21 days between  
41 applications). Programs were evaluated in terms of RLB incidence and number  
42 of applications. The program based on the model with periodic fungicide  
43 applications was similarly effective as the standard, resulting only in a 2.6%  
44 higher RLB incidence but with fewer applications (three to four, compared with  
45 seven in the standard). When setting the frequency between applications by  
46 using the meteorological criteria, a higher reduction in the number of  
47 applications (two to three) was observed, while RLB incidence increased by  
48 roughly 16% in both programs. Therefore, the model developed in this study  
49 may represent a valuable tool towards a more sustainable fungicide  
50 schedule for the control of almond RLB in northeast Spain.

51 **INTRODUCTION**

52 Red leaf blotch (RLB) is one of the most important foliar diseases  
53 affecting almond (*Prunus dulcis* (Mill.) D.A. Webb) in the Mediterranean Basin  
54 and Middle East (Cannon 1996; Farr and Rossman 2022). The disease is  
55 endemic in these regions and to date has not been reported as occurring in  
56 other almond-growing areas in the world such as the USA or Australia (Farr and  
57 Rossman 2022). RLB is caused by the ascomycete *Polystigma amygdalinum*  
58 P.F. Cannon. The pathogen overwinters in almond leaf litter where the sexual  
59 stage is developed and ascospores are produced in perithecia. In spring, under  
60 favorable temperature and humidity conditions, and especially after rain events,  
61 mature ascospores are released and air-spread to eventually infect new almond  
62 leaves (Banihashemi 1990; Pons-Solé et al. 2023; Suzuki et al. 2008).  
63 Banihashemi (1990) showed that ascospore release in Iran begins at bloom  
64 (early March) and reaches the maximum at petal fall and the beginning of fruit  
65 set (late March to early April), whereas in Lebanon ascospore release can occur  
66 between February and mid-May (Saad and Masannat 1997). Similarly, the main  
67 infection period in Spain has been reported to be from March to mid-June  
68 (Zúñiga et al. 2020). Following infections, fungal stromata develop and RLB  
69 symptoms appear after a relatively long incubation period of 30 to 40 days in  
70 Iran and Lebanon (Banihashemi 1990; Saad and Masannat 1997), and from 35  
71 to 70 days in Spain (Zúñiga et al. 2020). First symptoms appear as pale  
72 yellowish spots on both leaf sides, turning into orange-reddish and finally dark  
73 brown. Lesion size increases with time and in late summer they may cover  
74 almost entirely the leaf surface. When disease severity is high, premature  
75 defoliation can be observed in summer (Cannon 1996; Habibi and Banihashemi

76 2016; Miarnau et al. 2021; Shabi 1997), with a subsequent decrease in tree  
77 photosynthetic activity and thus possibly affecting yield (López-López et al.  
78 2016). The occurrence of secondary infection cycles during the cropping  
79 season has not been confirmed, as conidia formed during summer in pycnidia  
80 are not infective and are thought to act as spermatia in the sexual reproduction  
81 of the pathogen (Cannon 1996; Habibi and Banihashemi 2016). Therefore, RLB  
82 is considered a monocyclic disease with a single inoculum source consisting of  
83 the perithecia formed in infected leaves fallen in the previous year.

84         Concerning the effect of meteorological conditions on the life cycle of *P.*  
85 *amygdalinum*, in Iran Ghazanfari and Banihashemi (1976) reported on the  
86 importance of winter temperatures below 10°C for perithecia maturation. More  
87 recently in Spain, Zúñiga et al. (2020) found that the meteorological conditions  
88 from October to January influence the total available ascospore amount for the  
89 next season. The authors found positive correlations between the total seasonal  
90 ascospore amounts and the mean relative humidity, the accumulated rainfall,  
91 the number of rainy days, and the number of days with mean temperature  
92 higher than 20°C recorded within this period. Recently, Pons-Solé et al. (2023)  
93 suggested that *P. amygdalinum* ascospore release may benefit from concurrent  
94 mild temperatures (between 10°C and 20°C) and the hydration of fallen leaves  
95 through humidity or rain. Regarding the relationships between meteorological  
96 variables and RLB disease development in Catalonia, Spain, Miarnau et al.  
97 (2021) observed that annual RLB incidence was positively correlated with the  
98 accumulated rainfall in spring (especially in April), while it was negatively  
99 correlated with high temperatures in spring (especially in May) and summer.

100           There are no known almond cultivars completely resistant to RLB,  
101 although several authors have observed differential levels of RLB susceptibility  
102 among cultivars (Heydarian and Moradi 2005; Miarnau et al. 2021; Ollero-Lara  
103 et al. 2019). This means that effective control strategies against RLB mainly  
104 rely on the protection of trees with fungicides. Regarding RLB control with  
105 fungicides, experiments on the efficacy of various plant protection products  
106 have been conducted in Iran (Amanifar 2017; Banihashemi 1990; Bayt Tork et  
107 al. 2014), reporting triforine and mancozeb as the most effective fungicides  
108 against RLB. Recently in Spain, Torguet et al. (2022) observed that, in general,  
109 systemic fungicides performed better than contact ones. Currently registered  
110 fungicides for RLB control in Spain are included in FRAC groups 3 (sterol  
111 biosynthesis inhibitors, i.e., difenoconazole), 7 (succinate dehydrogenase  
112 inhibitors, i.e., boscalid), and 11 (quinone outside inhibitors, i.e., pyraclostrobin  
113 and kresoxim-methyl) (FRAC 2022; MAPA 2022). To get effective disease  
114 control, five to nine fungicide applications are usually timed on a calendar  
115 basis each season, starting at petal fall and ending in summer (July to August)  
116 (Torguet et al. 2022). However, little research has been done on optimizing  
117 fungicide programs. Torguet et al. (2022) compared calendar-based programs  
118 (every 14, 21, or 31 days from petal fall) with meteorological-based programs  
119 (15 days after rainfalls over 15 mm and with 10 to 15°C as mean minimum  
120 temperature), proving that programs following those meteorological criteria were  
121 just as effective as those calendar-based but with fewer number of  
122 applications.

123           To be effective, fungicide applications against RLB must coincide with  
124 the infection period, defined by the presence of airborne ascospores,

125 susceptible host leaves, and favorable conditions for infection.  
126 Epidemiological models are a useful tool to predict the periods of higher risk of  
127 infection based on meteorological variables (De Wolf and Isard 2007), thus  
128 avoiding the direct quantification of inoculum in real-time conditions, which is  
129 methodologically and logistically difficult to achieve. Modeling approaches can  
130 be used together with action thresholds to develop decision support systems  
131 (DSSs) and optimize the management of plant diseases (Gent et al. 2013;  
132 Knight 1997). DSSs can serve as decision aids to schedule fungicide  
133 applications based on disease risk, so that the number of fungicide  
134 applications can be reduced without compromising disease control efficacy  
135 (Lázaro et al. 2021; Marimon et al. 2020). Reducing fungicide application  
136 frequency and overall use is desirable as it reduces the environmental impact  
137 and the economic cost of crop protection. In the European Union, this has been  
138 promoted by the European Commission through the European Green Deal and  
139 specifically the 'from farm to fork' strategy, which targets a reduction in the use  
140 of chemical pesticides by half in 2030 (European Commission 2020).

141 To our knowledge, no epidemiological models to predict RLB risk of  
142 infection are available. Therefore, we aimed to develop an epidemiological  
143 model for *P. amygdalinum* airborne inoculum dynamics under the cropping  
144 conditions in Catalonia, Northeast Spain, to optimize fungicide programs and  
145 contribute towards a more sustainable disease control. The specific objectives  
146 of this work were: i) to develop an epidemiological model to predict *P.*  
147 *amygdalinum* airborne ascospore availability based on meteorological variables,  
148 and ii) to evaluate the performance of the model in a DSS to schedule optimized  
149 fungicide programs for RLB management.

150

## 151 **MATERIALS AND METHODS**

### 152 **Experimental orchards**

153           The model was developed with data collected from 2019 to 2021 in an  
154 experimental almond orchard owned by IRTA (Institut de Recerca i  
155 Tecnologia Agroalimentàries) (orchard 1) and a commercial one (orchard 2).  
156 Model evaluation was carried out in 2022 in orchard 2 and three additional  
157 commercial orchards of similar characteristics (orchards 3 to 5). All orchards  
158 were located in Lleida province, Catalonia, NE Spain, within a radius of 26 km  
159 area (Table 1). RLB occurs naturally in all orchards, as it is a widespread  
160 disease in the study region (Miarnau et al. 2021). Orchards 1 to 3 were  
161 planted in alternating rows with various earlier and later-flowering cultivars, as it  
162 is common in this almond-growing region. All orchards were drip irrigated, and  
163 pruning, soil management, and fertilization were based on the Spanish  
164 Integrated Production Management practices (BOE 2002). Leaf litter was  
165 present in all orchards, and no products (e.g., urea) were applied to  
166 promote its decomposition. Weeds were controlled by mechanical  
167 methods since no herbicides were used during the experimental period.  
168 No fungicide treatments were applied in any of the orchards during the  
169 experiments, besides the applications corresponding to the model evaluation  
170 carried out in 2022 in orchards 2 to 5.

### 171 **RLB airborne inoculum dynamics**

172           A Hirst 7-day recording volumetric spore trap (Burkard Manufacturing Co.  
173 Ltd, Rickmansworth, Hertfordshire, UK) was placed in a central position in  
174 orchards 1 and 2, operating continuously from mid-February to mid-September



175 in 2019, 2020, and 2021. The airflow was set at 10 L min<sup>-1</sup>, with the intake  
176 orifice located at 0.45 m above the ground. Airborne particles were captured  
177 on a Melinex<sup>®</sup> 200 gauge (TEKRA, New Berlin, WI, USA) plastic tape, rotating  
178 at 2 mm h<sup>-1</sup> and previously coated with a layer of silicone solution (Lanzoni,  
179 Bologna, Italy). Tapes were processed to estimate the daily airborne ascospore  
180 concentration of *P. amygdalinum* according to the molecular methods described  
181 by Zúñiga et al. (2018). DNA was extracted using the E.Z.N.A<sup>®</sup> Plant DNA Kit  
182 (Omega Bio-Tek, Norcross, GA, USA), and real-time quantitative PCR (qPCR)  
183 was conducted in a Stepone<sup>™</sup> Real-Time PCR System thermal cycler (Life  
184 Technologies, Carlsbad, CA, USA), using the *P. amygdalinum* specific primer  
185 pair PamyI2F4/PamyI2R2 (Zúñiga et al. 2018). Daily concentration of  
186 ascospores (ascospores m<sup>-3</sup>) was calculated considering the daily air volume  
187 sunk by the spore trap. The yearly cumulative concentration of trapped  
188 ascospores was calculated for each orchard, as the total of daily ascospore  
189 concentrations. For the statistical analyses, the cumulative proportion of  
190 ascospores on a 0 to 1 scale was calculated on a daily basis, based on the daily  
191 concentration of ascospores and the yearly cumulative concentration of  
192 ascospores, for each orchard and year.

### 193 **Weather data**

194 For model development, daily accumulated rainfall, mean relative  
195 humidity (RH), and mean temperature were monitored from 2019 to 2021 in  
196 orchards 1 and 2 by automatic weather stations of the Meteorological Service of  
197 Catalonia (MeteoCat,  
198 <https://ruralcat.gencat.cat/web/guest/agrometeo.estacions>). The weather station  
199 in orchard 1 was located about 250 m away, while the closest weather station to

200 orchard 2 was located in Tàrrega (UTM 31T X = 347015, Y = 4614430), about 6  
 201 km away. From weather data, three new variables were calculated following  
 202 Rossi et al. (2009), based on the sums of the daily mean temperatures  
 203 above 0°C. These variables were: accumulated degree-days (ADD), ADD  
 204 considering vapor pressure deficit (ADDvpd), and ADD considering vapor  
 205 pressure deficit and rainfall (ADDwet), computed as follows:

$$206 \quad ADD_i = \sum_{j=biifix}^{N_i} T_j$$

$$207 \quad ADDvpd_i = \sum_{j=biifix}^{N_i} T_j \cdot VPD_j$$

$$208 \quad ADDwet_i = \sum_{j=biifix}^{N_i} T_j \cdot WET_j$$

209 where  $i$  and  $j$  are the subscripts for observations and days, respectively,  
 210 ranging between the biofix (January 1<sup>st</sup> each year) and the number of days  
 211 until time  $i$ ,  $N_i$ .  $T_j$  is the mean daily air temperature (°C) when  $T_j > 0$ ,  
 212 otherwise  $T_j = 0$ .  $VPD_j$  is a binary variable calculated as follows: when  
 213 vapor pressure deficit (vpd)  $\leq 4$  hPa,  $VPD_j = 1$ ; otherwise,  $VPD_j = 0$ , with  
 214 vpd calculated from temperature and relative humidity (rh, %) as shown:

$$215 \quad vpd_j = \left(1 - \frac{rh_j}{100}\right) \cdot 6.11 \cdot \exp\left(\frac{17.47 \cdot T_j}{239 + T_j}\right)$$

216 Finally,  $WET_j$  is a binary variable calculated as follows: when rainfall  $\geq 2$   
 217 mm and vpd  $\leq 4$  hPa,  $WET_j = 1$ , otherwise,  $WET_j = 0$ .

218 For the model evaluation in 2022, the same weather station in orchard 2  
 219 was used, while an additional wireless cellular data logger with rain, RH, and

220 temperature sensors (Em50, Decagon Devices, Pullman, WA, USA) was  
221 installed in each of orchards 3 to 5.

### 222 **Modeling the dynamics of airborne ascospores**

223 Beta regression was used to relate the cumulative proportion of captured *P.*  
224 *amygdalinum* ascospores to the fixed factors ADD, ADDvpd, and ADDwet due  
225 to the nature of the response variable, which assumes values in the open  
226 interval (0,1). The model was fitted using the data collected from 2019 to 2021  
227 in orchards 1 and 2 and it was parametrized in terms of the mean  $\mu$  and a  
228 dispersion parameter  $\Phi$  whereby the variance

$$229 \quad \sigma^2 = \frac{\mu(1 - \mu)}{1 + \Phi}$$

230 is dependent on the mean (Ferrari and Cribari-Neto 2004). Let  $Y_{ilk}$  ( $i = 1, \dots, n$ ;  $l$   
231  $= 1, \dots, L$ ;  $k = 1, \dots, K$ ) be the cumulative proportion of ascospores for the  $i$ th  
232 observation in location  $l$  and year  $k$ , with mean  $\mu_{ilk}$  and unknown precision  $\Phi$ .  
233 The mean ( $\mu_{ilk}$ ) was linked to the linear predictor using the logit function:

$$234 \quad \text{logit}(\mu_{ilk}) = \beta_0 + \sum_{j=1}^{N_\beta} \beta_j x_{jilk} + v_{lk}$$

235 where  $\beta_0$  is the intercept of the model,  $x_{jilk}$  are the fixed factors (i.e., ADD,  
236 ADDvpd, and ADDwet),  $\beta_j$  are the parameters for the fixed factors, and  $v_{lk}$   
237 represents an independent structured random effect for the year and orchard  
238 location. This random effect captures the heterogeneity and the variability  
239 that may exist between the  $l$  locations and the  $k$  years. To avoid zeros and  
240 ones, the response data were transformed as  $y_i^{new} = \frac{y_i \cdot (n-1) + 1/2}{n}$  where  $n$  is the  
241 sample size, as proposed by Smithson and Verkuilen (2006).

### 242 **DSS evaluation**

243 ***Fungicide application programs.*** According to Magarey and Sutton (2007), a  
244 commercial evaluation of a given model should test how well the model output  
245 can be used to predict the appropriate deployment of disease management  
246 measures. Usually, disease incidence and/or severity and the number of  
247 fungicide applications are compared between calendar-based and model-  
248 driven fungicide programs. In our case, different fungicide application  
249 programs were evaluated in 2022 in orchards 2 to 5 (Table 1). In orchards 2  
250 and 3, programs were assessed on cultivar 'Marinada' trees, whereas 'Guara'  
251 was the assessed cultivar in orchards 4 and 5. In each orchard, the trial had a  
252 randomized block design, with four experimental blocks and four-tree plots per  
253 evaluated program as experimental units. Five programs were evaluated: i)  
254 CAL: standard calendar-based program, with applications initiating at petal fall  
255 and repeated every 21 days to the end of July; ii) CAL+MET: like CAL, but  
256 applications were repeated with meteorological criteria (until seven days after  
257 rain episodes greater than 10 mm and with daily mean temperatures between  
258 10°C and 20°C; with a minimum frequency of 21 days between applications),  
259 as adapted from Torguet et al. (2022); iii) MOD: the model selected in this study  
260 was implemented in this program. Action thresholds of 10% and 65% predicted  
261 cumulative ascospores were chosen to start and finish fungicide applications,  
262 respectively, with a frequency between applications of 21 days; iv) MOD+MET:  
263 like MOD, but applications were repeated with the same meteorological criteria  
264 used in CAL+MET; and v) UTC: non-treated control. The 10% initial threshold  
265 was chosen considering the selected model's potential for overprediction  
266 at lower values, and to ensure that treatments would be initiated when  
267 new leaves were present. The 65% threshold was chosen to conclude

268 fungicide applications considering that the main infection period of *P.*  
269 *amygdalinum* in Spain has been reported to be from March to mid-June  
270 (Zúñiga et al. 2020), though airborne ascospores might be less present  
271 until the end of August.

272 The product used for all fungicide applications was Signum® (from BASF;  
273 active ingredients: Pyraclostrobin 6.7% + Boscalid 26.7%), applied at the label  
274 concentration of 1.0 kg ha<sup>-1</sup> (MAPA 2022). This fungicide was chosen because  
275 it was the only registered product for the control of RLB in 2022 in Spain  
276 (MAPA 2022) which showed good performance to control RLB in previous  
277 studies (Torguet et al. 2022). The fungicide was applied using a single nozzle  
278 sprayer Turbo 400 (Sirfran, Alicante, Spain) at 2 bars. The application volume  
279 was calibrated to approximately 1,000 L ha<sup>-1</sup>, which is a common commercial  
280 rate used in most Spanish almond-growing regions.

281 To evaluate the fungicide programs, we considered both the seasonal  
282 number of applications and the resulting RLB incidence at the end of the  
283 experimental period. RLB incidence was assessed in early August 2022 as  
284 described by Miarnau et al. (2021). In each experimental unit, 100 leaves (50  
285 per each of the two central trees) were arbitrarily selected from new shoots at  
286 different heights and orientations located in the outer canopy. RLB incidence  
287 was recorded as the number of diseased leaves (i.e., leaves showing at least  
288 one identifiable RLB lesion) out of the total evaluated leaves.

289 **Model definition.** Binomial logistic regression was used to estimate the RLB  
290 incidence for each of the considered fungicide programs (CAL, CAL+MET,  
291 MOD, MOD+MET, and UTC). Additionally, the almond cultivar ('Guara' (GUA)  
292 vs 'Marinada' (MAR)) was also included in the model as a fixed effect. The

293 model was fitted using the data collected in 2022 in orchards 2 to 5. The  
 294 number of diseased leaves,  $Z_{ilk}$  ( $i = 1, \dots, n; l = 1, \dots, L; k = 1, \dots, K$ ) for the  $i$ th  
 295 observation within the block  $l$  of the orchard  $k$ , out of a total of  $n_{ilk}$  leaves  
 296 analyzed, was assumed to follow a binomial distribution with unknown  
 297 probability of disease,  $\theta_{ilm}$  (i.e., RLB incidence).

$$298 \quad Z_{ilm} \sim \text{Binomial}(n_{ilm}, \theta_{ilm})$$

299 RLB incidence ( $\theta_{ilk}$ ) was linked to the linear predictor using the logit function:

$$300 \quad \text{logit}(\theta_{ilk}) = \alpha_0 + \sum_{j=1}^{N_\alpha} \alpha_j x_{jilk} + u_k + w_{l:k}$$

301 where  $\alpha_0$  is the intercept of the model, which captures the effect of the  
 302 untreated control-cultivar 'Guara' (UTC-GUA),  $x_{jilk}$  are the fixed factors (i.e.,  
 303 CAL, CAL+MET, MOD, MOD+MET, MAR),  $\alpha_j$  are the parameters for the fixed  
 304 factors. In addition, the model includes two random effects:  $u_k$  as an  
 305 independent random effect to capture the variability between the  $k$  orchards,  
 306 and  $w_{l:k}$  as a nested random effect between the block  $l$  within the orchard  $k$ ,  
 307 which captures variability between the  $l$  blocks distinguishing blocks within the  
 308 same orchard.

### 309 **Model inference**

310 For both models (i.e., the beta regression and the binomial regression)  
 311 inference was carried out using Bayesian statistics with integrated nested  
 312 Laplace approximations (INLA) by means of the 'R-INLA' package for R (Rue et  
 313 al. 2009). For the beta regression model, the R code provided by Martínez-  
 314 Minaya et al. (2021) was adapted. All statistical analyses were implemented in  
 315 R software version 4.2.0 (R Core Team 2022).

316 Both inference processes were set under weakly independent prior  
317 scenarios. Specifically, for the beta regression model, parameters associated to  
318 the fixed effects were defined considering vague Gaussian prior distributions  
319  $\beta_j \sim N(0, \tau_\beta = 10^{-3})$ , and an independent Gaussian distribution for the random  
320 effect location-year  $v_{lk} \sim N(0, \tau_v = 1/\sigma_v^2)$ . In this model,  $\tau_v$  and  $\Phi$  were  
321 considered hyperparameters and their corresponding priors were defined as  
322  $\tau_v \sim \text{PC} - \text{prior}(5, 0.01)$  and  $\Phi \sim \text{Ga}(1, 0.1)$  respectively. Pearson correlation  
323 coefficients between fixed factors were calculated, and those models  
324 considering fixed factors with  $|r| > 0.7$  were not further considered to avoid  
325 potential problems of multicollinearity (Dormann et al. 2013). For the binomial  
326 regression, parameters associated to the fixed effects were also defined  
327 considering vague Gaussian prior distributions  $\alpha_j \sim N(0, \tau_\alpha = 10^{-3})$ , and two  
328 independent Gaussian distributions for the two random effects,  $u_k \sim N(0, \tau_u =$   
329  $1/\sigma_u^2)$  and  $w_{l:k} \sim N(0, \tau_w = 1/\sigma_w^2)$ . In this model,  $\tau_u$  and  $\tau_w$  were considered  
330 hyperparameters and their corresponding priors were defined as  
331  $\tau_u \sim \text{Ga}(0.001, 0.001)$  and  $\tau_w \sim \text{Ga}(0.001, 0.001)$ , respectively.

332 For both the beta regression and the binomial regression analysis, all  
333 possible combinations of their respective initial components were  
334 evaluated. The total number of combinations was  $2^k$ , with  $k$  denoting the  
335 number of components in the linear predictor, including random effects.  
336 The main objective was to identify the most parsimonious model that  
337 offered optimal explanatory and predictive performance. The best model  
338 was selected according to the deviance information criterion (DIC)  
339 (Spiegelhalter et al. 2002), the widely applicable information criterion (WAIC)  
340 (Watanabe 2010), and the mean logarithmic conditional predictive ordinate

341 (LCPO) (Roos and Held 2011), by selecting the model with the lowest values of  
342 DIC, WAIC, and LCPO. As a rule of thumb, if two models differed in DIC by  
343 more than 3, the one with the smaller DIC was preferred (Spiegelhalter et al.  
344 2002). In the case of WAIC and LCPO, there is no rule of thumb about how  
345 much this difference should be. When no meaningful differences were observed  
346 between models, the parsimony criterion was applied and the model with fewer  
347 covariates was finally selected.

348 For the beta regression selected model, median values of the posterior  
349 predictive distribution were linearly regressed against the observed values, and  
350 the coefficient of determination ( $R^2$ ), mean absolute error (MAE), and root mean  
351 square error (RMSE) were further calculated.

352

## 353 **RESULTS**

### 354 **RLB airborne inoculum dynamics and weather summary**

355 In orchard 1, yearly cumulative concentration of ascospores in 2019, 2020,  
356 and 2021 were estimated by qPCR to be 1043, 506, and 30 ascospores  $m^{-3}$ ,  
357 respectively. In orchard 2, the corresponding cumulative concentration of  
358 ascospores were 6044, 581, and 111 ascospores  $m^{-3}$ , respectively. In orchard  
359 1, 90% of ascospore detection was reached between mid-August and mid-  
360 September in 2019 and 2020, but in early May in 2021. In orchard 2, 90% of  
361 ascospore detection was reached between late May and early July in all  
362 monitored years.

363 During the study period in orchard 1, annual mean temperature ranged  
364 from 14.6°C in 2021 to 14.9°C in 2019, the number of days with VPD  $\leq$  4 hPa  
365 ranged from 131 in 2019 to 164 in 2020 and 2021, and the number of days with



366 rainfall  $\geq 0.2$  mm ranged from 60 in 2019 to 90 in 2020. In orchard 2, annual  
367 mean temperature ranged from 14.3°C in 2021 to 14.6°C in 2019 and 2020, the  
368 number of days with VPD  $\leq 4$  hPa ranged from 132 in 2019 to 168 in 2020, and  
369 the number of days with rainfall  $\geq 0.2$  mm ranged from 76 in 2019 and 2021 to  
370 92 in 2020. Regarding the ADD-derived variables (Fig. 1), annual ADD in  
371 orchard 1 ranged from 5324°C-days to 5448°C-days (in 2021 and 2019,  
372 respectively); annual ADDv<sub>pd</sub> ranged from 1051°C-days to 1433°C-days (in  
373 2019 and 2021, respectively); and ADD<sub>wet</sub> ranged from 389°C-days to 605°C-  
374 days (in 2019 and 2020, respectively). In orchard 2, annual ADD ranged from  
375 5242°C-days to 5358°C-days (in 2021 and 2020, respectively); annual ADDv<sub>pd</sub>  
376 ranged from 979°C-days to 1417°C-days (in 2019 and 2020, respectively); and  
377 ADD<sub>wet</sub> ranged from 389°C-days to 557.0°C-days (in 2021 and 2020,  
378 respectively).

### 379 **Modeling the dynamics of airborne ascospores**

380 The explored models for the cumulative proportion of ascospores of *P.*  
381 *amygdalinum* are ranked in Table 2 based on their DIC, WAIC, and LCPO  
382 values. Considering that the Pearson correlation coefficient between ADDv<sub>pd</sub>  
383 and ADD<sub>wet</sub> in the ascospore monitoring period was  $|r| = 0.92$ , models  
384 including both variables were not considered. Thus, the selected model  
385 included the fixed effects ADD and ADD<sub>wet</sub>, and the random effect for the year-  
386 location ( $\nu$ ).

387 In the selected model, the parameter for the fixed effect ADD had a  
388 median posterior distribution of 0.086 with a 95% credible interval (CrI) (0.077,  
389 0.094), while the parameter for the fixed effect ADD<sub>wet</sub> had a median posterior  
390 distribution of 1.107 with a 95% CrI (0.982, 1.235). None of the credible

391 intervals were overlapping with zero (Table 3). Therefore, the two fixed effects  
392 had positive effects on the expected cumulative proportion of *P. amygdalinum*  
393 airborne ascospores. The posterior distribution of the two hyperparameters was  
394 also computed (Table 3). The median posterior distribution of the dispersion  
395 parameter  $\Phi$  was 3.048, while in the case of the precision of the random  
396 effect  $\tau_v$  it was 0.993. This indicates that it is important to consider the random  
397 effect in the model, as it explains some of the variability that fixed effects cannot  
398 explain. When computing the linear regression of the observed values against  
399 the median posterior predictive distribution, it accounted for 78% of the total  
400 variance ( $R^2 = 0.78$ ), with a slope of 0.736 and an intercept of 0.143 (Fig. 2).  
401 The MAE for this model was 0.141, and the RMSE was 0.180.

402           Considering the median posterior distribution (Fig. 3), 10% of *P.*  
403 *amygdalinum* ascospores were captured from 465 to 920 ADD and from 60 to  
404 105 ADDwet, corresponding from 3 March to 19 April. At the other extreme,  
405 90% of ascospores were captured from 1790 to 3745 ADD and from 155 to 305  
406 ADDwet, corresponding from 6 June to 29 August.

#### 407 DSS evaluation

408           The explored models for the RLB incidence are ranked in Supplementary  
409 Table S1 based on their DIC, WAIC, and LCPO values. The selected model  
410 included as fixed effects only those related to the fungicide programs, and the  
411 nested random effect ( $w$ ) block:orchard. The covariate associated with the  
412 cultivar did not significantly improve the explanatory behavior of the model  
413 (Supplementary Table S1).

414           From the posterior distribution of the fixed parameters (Supplementary  
415 Table S2) of the selected model, the expected RLB disease incidence for each

416 of the evaluated fungicide programs across all the experimental orchards was  
417 computed. The median RLB incidence for the UTC was 82.8%, 95% CrI  
418 (75.3%, 88.3%). On the other extreme, the median RLB incidence in the CAL  
419 program was 2.4%, 95% CrI (1.4%, 4.0%), whereas in the rest of assessed  
420 programs it ranged from 5.0%, 95% CrI (3.1%, 8.1%) in MOD to 19.0%, 95%  
421 CrI (12.6%, 27.7%) in CAL+MET (Fig. 4).

422 The posterior distributions of the estimated differences in RLB incidence  
423 between the fungicide programs (Table 4) showed that all programs led to a  
424 substantial reduction in RLB incidence compared to the UTC with probabilities  
425 of these differences as being negative equal to one ( $P(<0) = 1$ ). Specifically, on  
426 average over all orchards, the CAL program led to a reduction in RLB incidence  
427 of -80.4%, 95% CrI (-84.7%, -73.8%) while the CAL+MET program showed a  
428 reduction of -63.3%, 95% CrI (-66.2%, -73.8%), compared to UTC. Similarly,  
429 the MOD program showed a reduction in RLB incidence of -77.6%, 95% CrI  
430 (-81.0%, -72.0%) while the MOD+MET led to a reduction of -64.4%, 95% CrI  
431 (-66.9%, -60.2%), also compared to UTC.

432 All the programs including the model and/or the meteorological criteria  
433 (CAL+MET, MOD, MOD+MET) when compared with CAL, resulted in RLB  
434 incidence increases as follows: +16.6%, 95% CrI (11.0%, +24.2%) in  
435 CAL+MET; +2.6%, 95% CrI (+1.20%, +4.9%) in MOD; and +16.0%, 95% CrI  
436 (10.5%, +23.4%) in MOD+MET (Table 4). Hence, the levels of disease  
437 incidence between MOD and CAL programs were those that differed the lowest  
438 (+2.6%). The credible interval for the estimated difference between MOD+MET  
439 and CAL+MET overlapped zero, thus indicating that no substantial difference  
440 on RLB incidence was detected between these programs.

441 Concerning the total number of fungicide applications, information is  
442 summarized in Table 5. The first application was carried out between 17 March  
443 and 4 April, while the last was between 21 April and 29 July, depending on the  
444 fungicide program. On average,  $7.00 \pm 0.0$  (mean  $\pm$  std. error) seasonal  
445 applications were made with the CAL standard fungicide program,  $3.75 \pm 0.5$   
446 applications with the MOD program (a 46% reduction compared to CAL), and  
447  $2.25 \pm 0.5$  applications with the MOD+MET and CAL+MET fungicide programs  
448 (a 68% reduction).

449

## 450 **DISCUSSION**

451 In this study, a Bayesian beta regression framework was implemented to  
452 model the dynamics of *P. amygdalinum* airborne ascospores in Lleida region,  
453 NE Spain. The beta regression avoids traditional data transformations as it  
454 assumes that the response variable follows a beta distribution, which is flexible  
455 for modeling proportions as it is defined by only two parameters (Ferrari and  
456 Cribari-Neto 2004). This modeling approach was proposed by Martínez-Minaya  
457 et al. (2021) to describe ascospore dynamics of *Plurivorosphaerella nawae*. To  
458 our knowledge, the beta regression model reported here is the first  
459 epidemiological model developed to predict the airborne inoculum dynamics of  
460 *P. amygdalinum*. The model was further used to design and evaluate a DSS to  
461 optimize fungicide application programs for RLB management.

462 Modeling was performed using the combination of three types of  
463 accumulated degree-days variables (ADD, ADDvpd, and ADDwet) since several  
464 biological systems, such as ascospore maturation and release, have been  
465 reported to be dependent on thermal time accumulation (Lovell et al. 2004;

466 Martínez-Minaya et al. 2021; Rossi et al. 2009; Spotts and Cervantes 1994).  
467 January 1 was chosen as the biofix to start degree-days accumulation for being  
468 a fixed date in which, in our conditions, almond leaf fall is completed and mature  
469 perithecia stages are still not present in infected leaf litter (Zúñiga et al. 2020).  
470 In our selected model, ADD and ADDwet were the variables driving *P.*  
471 *amygdalinum* airborne ascospore availability. Both variables had a continuous  
472 positive effect on the predicted variable, with the coefficient of ADDwet being  
473 greater. The inability to consider both ADDvdpd and ADDwet variables in the  
474 same model because of their high correlation showed that ADDwet was more  
475 relevant in the model than ADDvdpd, thus highlighting the importance of water  
476 availability on the *P. amygdalinum* ascospore development and release along  
477 the season. This is consistent with previous findings reported in Spain by  
478 Zúñiga et al. (2020), who found that the seasonal amount of available  
479 ascospores was positively correlated with the accumulated rainfall in January.  
480 Moreover, Miarnau et al. (2021) reported a positive correlation between annual  
481 RLB incidence and accumulated spring rainfall, which would also support the  
482 findings of this study. More recently, Pons-Solé et al. (2023) suggested that *P.*  
483 *amygdalinum* inoculum release may benefit from concurrent mild temperatures  
484 (between 10 and 20°C) and the hydration of fallen leaves, associated with  
485 humidity and rain variables. Torguet et al. (2022) also found that it was efficient  
486 to program RLB fungicide applications after rain events over 15 mm with 10 to  
487 15°C as minimum temperature, thus suggesting a relationship between these  
488 meteorological conditions and airborne inoculum availability and subsequent  
489 infections. Similarly, wetness and temperature have been noted as drivers for  
490 ascospore development and dispersal in other ascomycete pathogens with an

491 overwintering stage in leaf litter. Rossi et al. (2009) regressed the cumulative  
492 proportion of *Venturia pyrina* trapped ascospores against physiological time and  
493 found the best fit when using ADDwet. For *P. nawae*, ADD and ADDvpd were  
494 useful to model the dynamics of ascospore production in leaf litter, also  
495 suggesting that dew resulting from low VPD may favor ascospore development  
496 in the absence of rain (Martínez-Minaya et al. 2021).

497         Additionally, our selected model incorporated a random effect  
498 associated with the year and the location suggesting that, as expected, there  
499 were additional unmeasured sources of variability determining the availability of  
500 *P. amygdalinum* airborne ascospores. These variability sources may be related  
501 to several factors, such as infection dynamics among years or intrinsic  
502 characteristics of the locations and the almond cultivars present there or  
503 nearby. Nevertheless, the model showed high goodness of fit and accounted for  
504 78% of the total variance of the observed values, which is relevant considering  
505 the above-mentioned sources of variability, as well as the high variability  
506 observed between the yearly cumulative concentration of ascospores across  
507 the studied orchards and years. Also, it is worth noting the model's potential  
508 for overprediction at lower values and underprediction at higher values,  
509 traits that were considered when defining the DSS action thresholds.

510         The performance of the predictive model in a DSS was evaluated to  
511 optimize fungicide programs against RLB in 2022. The model was used to  
512 predict the beginning and the end of the airborne ascospore availability period,  
513 thus avoiding the time- and resource-consuming quantification of ascospores  
514 through molecular or microscopy tools, and thus determining the period in which  
515 trees must be protected. Thresholds of 10% and 65% of predicted cumulative

516 proportion of ascospores were proposed to start and finish fungicide  
517 applications, respectively, considering the median posterior predictive  
518 distribution of the model. In addition, we compared repeating applications  
519 every 21 days (as label recommended) or following specific meteorological  
520 criteria (until 7 days after rain episodes greater than 10 mm and with daily mean  
521 temperatures between 10 and 20°C, with a minimum frequency of 21 days).  
522 This second criterion, included in the CAL+MET and MOD+MET programs  
523 tested here, was adapted from that reported in Torguet et al. (2022), and  
524 additionally considering the recent findings obtained by Pons-Solé et al. (2023).  
525 In short, this criterion considers that *P. amygdalinum* ascospore release  
526 benefits from mild temperatures and the hydration of fallen leaves.

527 A single fungicide was used during the evaluation of fungicide programs,  
528 as the aim of our work was to determine the program-associated efficacies  
529 rather than the efficacy of the product itself. Signum® is a systemic product with  
530 preventive activity that showed good performance (75-95% efficacy) in a  
531 previous study (Torguet et al. 2022). Nevertheless, fungicide alternation should  
532 be rigorously observed when implementing DSSs in commercial orchards for  
533 RLB control, to limit the risk of developing pathogen resistance (Brent and  
534 Hollomon 2007). **Further research would be necessary to validate our  
535 findings when using other fungicide products including their alternation.**

536 Regarding the duration of the fungicide programs, it was observed that  
537 the main difference between the standard calendar-based program and the  
538 other evaluated programs was the timing of the last applications. Our results  
539 suggest that extending the protection period until mid-summer, as has been  
540 recommended for decades (Torguet et al. 2022), was not essential to show

541 good efficacy against RLB in 2022. The predictive model and action thresholds  
542 proposed here, as discussed below, can help to narrow the duration of fungicide  
543 programs which, in turn, would coincide with the RLB infection period previously  
544 described in Catalonia (Zúñiga et al. 2020). Additional research should be  
545 done to validate or adapt the proposed thresholds in different  
546 geographical contexts.

547 The efficiency of the tested programs was compared in terms of RLB  
548 control and number of seasonal applications. The observed levels of RLB  
549 incidence in the UTC during the experimental period were high, comparable to  
550 previous studies in the same region (Miarnau et al. 2021; Torguet et al. 2022),  
551 thus allowing the comparison between the four tested fungicide programs  
552 regarding RLB control. All the tested programs substantially reduced disease  
553 incidence as compared to the UTC. The standard CAL resulted in the lowest  
554 RLB incidence (median value of 2.4%), followed by the fungicide program that  
555 includes the predictive model (MOD) (median value of 5.0%) to establish the  
556 period in which trees must be protected. For the programs in which  
557 applications were repeated following specific meteorological criteria  
558 (CAL+MET and MOD+MET), the estimated RLB incidences were higher  
559 (median values of 19.0% and 18.4%, respectively). Nevertheless, the RLB  
560 control obtained with the CAL+MET and MOD+MET fungicide programs was  
561 still high and comparable to those reported by Torguet et al. (2022) with  
562 calendar-based applications (10% to 40% incidence in their study).

563 Besides, we observed great differences in the seasonal number of  
564 fungicide applications. We found that higher levels of disease control were  
565 associated with higher number of fungicide applications. On average, 7



566 applications were applied in the CAL standard program, whereas only 3.75  
567 applications in the MOD, and 2.25 applications in the CAL+MET and  
568 MOD+MET fungicide programs. When evaluating CAL+MET and MOD+MET  
569 fungicide programs, the 68% reduction in the number of applications led to an  
570 increase in RLB incidence of +16.6% and +16.0%, respectively, compared with  
571 the CAL standard program. However, the 46% reduction in the number of  
572 applications obtained with the MOD program resulted only in a RLB incidence  
573 increase of +2.6%. Hence, despite this relatively low increase in RLB incidence,  
574 we consider that the resulting reduction in the number of fungicide applications  
575 described in this work is noteworthy. Further research would be needed to  
576 untangle and quantify the relationship between low RLB levels and nut yield, to  
577 determine which disease thresholds farmers can assume without compromising  
578 almond production, and therefore decide the optimal fungicide strategy.

579 The results of the current research contribute towards the use of more  
580 sustainable fungicide programs against almond RLB disease in northeast  
581 Spain, and specifically the European Green Deal target of reducing by half the  
582 use of chemical pesticides by 2030 (European Commission 2020).

583

#### 584 **ACKNOWLEDGEMENTS**

585 The authors acknowledge the technical support from IRTA staff: Guillem  
586 Martínez, Robert Oró, Jesús Ortiz, Silvia Burillo, and Lourdes Zazurca.

587

#### 588 **DATA AVAILABILITY STATEMENT**

589 The data that support the findings of this study are openly available in CORA  
590 (Catalan Open Research Area – Repositori de Dades de Recerca) at  
591 <https://doi.org/10.34810/data237>.

592

### 593 **CONFLICT OF INTERESTS**

594 The authors declare no potential conflict of interests.

595

### 596 **LITERATURE CITED**

597 Amanifar, N. 2017. Evaluation of the efficiency of two fungicides on the control  
598 of almond leaf blotch disease on two cultivars in along Zayanderood. J.  
599 Plant Prot. 31:166-171.

600 Banihashemi, Z. 1990. Biology and control of *Polystigma ochraceum*, the cause  
601 of almond red leaf blotch. Plant Pathol. 39:309-315.

602 Bayt Tork, D., Taherian, M., and Divan, R. 2014. Evaluation of some fungicides  
603 for controlling almond red leaf blotch (*Polystigma amygdalinum*). Int. J.  
604 Adv. Biol. Biomed. Res. 4:1011-1016.

605 BOE. 2002. Real decreto 1201/2002, de 20 de noviembre, por el que se regula  
606 la producción integrada de productos agrícolas. Boletín Oficial del  
607 Estado, Madrid, Spain. <https://www.boe.es/eli/es/rd/2002/11/20/1201>

608 Brent, K. J., and Hollomon, D. W. 2007. Fungicide resistance in crop  
609 pathogens: how can it be managed? 2nd ed. Fungicide Resistance  
610 Action Committee, Brussels, Belgium.

611 Cannon, P. F. 1996. Systematics and diversity of the Phyllachoraceae  
612 associated with Rosaceae, with a monograph of *Polystigma*. Mycol. Res.  
613 100:1409-1427.

614 De Wolf, E. D., and Isard, S. A. 2007. Disease cycle approach to plant disease  
615 prediction. *Annu. Rev. Phytopathol.* 45:203-220.

616 Dormann, C. F., Elith, J., Bacher, S., Buchmann, C., Carl, G., Carré, G.,  
617 Marquéz, J. R., Gruber, B., Lafourcade, B., Leitão, P. J., Münkemüller,  
618 T., McClean, C., Osborne, P. E., Reineking, B., Schröder, B., Skidmore,  
619 A. K., Zurell, D., and Lautenbach, S. 2013. Collinearity: a review of  
620 methods to deal with it and a simulation study evaluating their  
621 performance. *Ecography* 36:27-46.

622 European Commission. 2020. Communication from the Commission to the  
623 European Parliament, the Council, the European Economic and Social  
624 Committee and the Committee of the Regions: A Farm to Fork Strategy  
625 for a fair, healthy and environmentally-friendly food system. E.  
626 Commission, ed., COM(2020) 381 final. [https://eur-lex.europa.eu/legal-](https://eur-lex.europa.eu/legal-content/EN/TXT/?uri=CELEX:52020DC0381)  
627 [content/EN/TXT/?uri=CELEX:52020DC0381](https://eur-lex.europa.eu/legal-content/EN/TXT/?uri=CELEX:52020DC0381)

628 Farr, D. F., and Rossman, A. Y. 2022. Fungal Databases, U.S. National Fungus  
629 Collections, ARS, USDA.

630 Felipe, A. J. 1977. Almendro: estados fenológicos. *Inf. Téc. Econ. Agrar.* 27:8-9.

631 Ferrari, S. L. P., and Cribari-Neto, F. 2004. Beta regression for modelling rates  
632 and proportions. *J. Appl. Stat.* 31:799-815.

633 Fungicide Resistance Action Committee (FRAC) 2022. FRAC Code List  
634 ©\*2022: Fungal control agents sorted by cross resistance pattern and  
635 mode of action (including coding for FRAC Groups on product labels).  
636 [https://www.frac.info/docs/default-source/publications/frac-code-list/frac-](https://www.frac.info/docs/default-source/publications/frac-code-list/frac-code-list-2022--final.pdf?sfvrsn=b6024e9a_2)  
637 [code-list-2022--final.pdf?sfvrsn=b6024e9a\\_2](https://www.frac.info/docs/default-source/publications/frac-code-list/frac-code-list-2022--final.pdf?sfvrsn=b6024e9a_2)

638 Gent, D. H., Mahaffee, W. F., McRoberts, N., and Pfender, W. F. 2013. The use  
639 and role of predictive systems in disease management. *Annu. Rev.*  
640 *Phytopathol.* 51:267-289.

641 Ghazanfari, J., and Banihashemi, Z. 1976. Factors influencing ascocarp  
642 formation in *Polystigma ochraceum*. *Trans. Br. Mycol. Soc.* 66:401-406.

643 Habibi, A., and Banihashemi, Z. 2016. Mating system and role of  
644 pycnidiospores in biology of *Polystigma amygdalinum*, the causal agent  
645 of almond red leaf blotch. *Phytopathol. Mediterr.* 55:98-108.

646 Heydarian, A., and Moradi, H. 2005. Relative resistance of selected almond  
647 cultivars to the causal agent of red leaf blotch disease, in Chahar mahal-  
648 va-Bakhtiari province. *Iran. J. Plant Pathol.* 41:157-169.

649 Knight, J. D. 1997. The role of decision support systems in integrated crop  
650 protection. *Agric. Ecosyst. Environ.* 64:157-163.

651 Lázaro, E., Makowski, D., and Vicent, A. 2021. Decision support systems halve  
652 fungicide use compared to calendar-based strategies without increasing  
653 disease risk. *Commun. Earth Environ.* 2:224.

654 López-López, M., Calderón, R., González-Dugo, V., Zarco-Tejada, P., and  
655 Fereres, E. 2016. Early detection and quantification of almond red leaf  
656 blotch using high-resolution hyperspectral and thermal imagery. *Remote*  
657 *Sens.* 8:276.

658 Lovell, D. J., Powers, S. J., Welham, S. J., and Parker, S. R. 2004. A  
659 perspective on the measurement of time in plant disease epidemiology.  
660 *Plant Pathol.* 53:705-712.

661 Magarey, R. D., and Sutton, T. B. 2007. How to create and deploy infection  
662 models for plant pathogens. Pages 3-25 in: *General concepts in*

663 integrated pest and disease management. A. Ciancio and K. G. Mukerji,  
664 eds. Springer, Dordrecht, The Netherlands.

665 MAPA. 2022. Registro de Productos Fitosanitarios.  
666 [https://www.mapa.gob.es/es/agricultura/temas/sanidad-](https://www.mapa.gob.es/es/agricultura/temas/sanidad-vegetal/productos-fitosanitarios/fitos.asp)  
667 [vegetal/productos-fitosanitarios/fitos.asp](https://www.mapa.gob.es/es/agricultura/temas/sanidad-vegetal/productos-fitosanitarios/fitos.asp)

668 Marimon, N., Eduardo, I., Martínez-Minaya, J., Vicent, A., and Luque, J. 2020. A  
669 decision support system based on degree-days to initiate fungicide spray  
670 programs for peach powdery mildew in Catalonia, Spain. *Plant Dis.*  
671 104:2418-2425.

672 Martínez-Minaya, J., Conesa, D., López-Quílez, A., Mira, J. L., and Vicent, A.  
673 2021. Modeling inoculum availability of *Plurivorosphaerella nawae* in  
674 persimmon leaf litter with Bayesian beta regression. *Phytopathology*  
675 111:1184-1192.

676 Miarnau, X., Zazurca, L., Torguet, L., Zúñiga, E., Batlle, I., Alegre, S., and  
677 Luque, J. 2021. Cultivar susceptibility and environmental parameters  
678 affecting symptom expression of red leaf blotch of almond in Spain. *Plant*  
679 *Dis.* 105:940-947.

680 Ollero-Lara, A., Agustí-Brisach, C., Lovera, M., Roca, L. F., Arquero, O., and  
681 Trapero, A. 2019. Field susceptibility of almond cultivars to the four most  
682 common aerial fungal diseases in southern Spain. *Crop Protect.* 121:18-  
683 27.

684 Pons-Solé, G., Miarnau, X., Torguet, L., Lázaro, E., Vicent, A., and Luque, J.  
685 2023. Airborne inoculum dynamics of *Polystigma amygdalinum* and  
686 progression of almond red leaf blotch disease in Catalonia, NE Spain.  
687 *Ann. Appl. Biol.* DOI: <https://www.doi.org/10.1111/aab.12831>

688 R Core Team. 2022. R: A language and environment for statistical computing. R  
689 Foundation for Statistical Computing, Vienna, Austria.

690 Roos, M., and Held, L. 2011. Sensitivity analysis in Bayesian generalized linear  
691 mixed models for binary data. *Bayesian Anal.* 6:259–278.

692 Rossi, V., Salinari, F., Pattori, E., Giosuè, S., and Bugiani, R. 2009. Predicting  
693 the dynamics of ascospore maturation of *Venturia pirina* based on  
694 environmental factors. *Phytopathology* 99:453-461.

695 Rue, H., Martino, S., and Chopin, N. 2009. Approximate Bayesian inference for  
696 latent Gaussian models by using integrated nested Laplace  
697 approximations. *J. R. Statist. Soc. B* 71:319-392.

698 Saad, A. T., and Masannat, K. 1997. Economic importance and cycle of  
699 *Polystigma ochraceum*, causing red leaf blotch disease of almond, in  
700 Lebanon. *EPPO Bulletin* 27:481-485.

701 Sakar, E. H., El Yamani, M., Boussakouran, A., and Rharrabti, Y. 2019.  
702 Codification and description of almond (*Prunus dulcis*) vegetative and  
703 reproductive phenology according to the extended BBCH scale. *Sci.*  
704 *Hortic.* 247:224-234.

705 Shabi, E. 1997. Disease management of the almond pathogens *Glomerella*  
706 *cingulata*, *Polystigma ochraceum* and *Tranzschelia pruni-spinosae*.  
707 *EPPO Bulletin* 27:479-480.

708 Smithson, M., and Verkuilen, J. 2006. A better lemon squeezer? Maximum-  
709 likelihood regression with beta-distributed dependent variables. *Psychol.*  
710 *Methods* 11:54–71.

- 711 Spiegelhalter, D. J., Best, N. G., Carlin, B. P., and Van der Linde, A. 2002.  
712 Bayesian measures of model complexity and fit. *J. R. Statist. Soc. B*  
713 64:583–639.
- 714 Spotts, R. A., and Cervantes, L. A. 1994. Factors affecting maturation and  
715 release of ascospores of *Venturia pirina* in Oregon. *Phytopathology*  
716 88:260-264.
- 717 Suzuki, Y., Tanaka, K., Hatakeyama, S., and Harada, Y. 2008. *Polystigma*  
718 *fulvum*, a red leaf blotch pathogen on leaves of *Prunus* spp., has the  
719 *Polystigmina pallescens* anamorph/andromorph. *Mycoscience* 49:395-  
720 398.
- 721 Torguet, L., Zazurca, L., Martínez, G., Pons-Solé, G., Luque, J., and Miarnau,  
722 X. 2022. Evaluation of fungicides and application strategies for the  
723 management of the red leaf blotch disease of almond. *Horticultrae*  
724 8:501.
- 725 Watanabe, S. 2010. Asymptotic equivalence of Bayes cross validation and  
726 widely applicable information criterion in singular learning theory. *J.*  
727 *Mach. Learn. Res.* 11:3571-3594.
- 728 Zúñiga, E., León, M., Berbegal, M., Armengol, J., and Luque, J. 2018. A qPCR-  
729 based method for detection and quantification of *Polystigma*  
730 *amygdalinum*, the cause of red leaf blotch of almond. *Phytopathol.*  
731 *Mediterr.* 57:257-268.
- 732 Zúñiga, E., Romero, J., Ollero-Lara, A., Lovera, M., Arquero, O., Miarnau, X.,  
733 Torguet, L., Trapero, A., and Luque, J. 2020. Inoculum and infection  
734 dynamics of *Polystigma amygdalinum* in almond orchards in Spain. *Plant*  
735 *Dis.* 104:1239-1246.

736 **TABLES**

737 **Table 1.** Characteristics of the almond orchards included in this study, and  
 738 years corresponding to *Polystigma amygdalinum* ascospore monitoring and  
 739 model development and evaluation

Orchard	Location	UTM coordinates (WGS 84, 31 T)		Plantation year	Cultivar	Rootstock	Tree spacing	Model development (ascospore monitoring)	Model evaluation
		X	Y						
1	Les Borges Blanques	320870	4597530	2009	Tarraco, Marinada <sup>a</sup>	GF-677	4 x 2 m	2019-2021	-
2	Vilagrassa	341313	4612125	2007	Tarraco, Marinada, Vairo, Belona <sup>a</sup>	GF-677	7 x 6 m	2019-2021	2022
3	Lleida	294423	4613174	2007	Tarraco, Marinada <sup>a</sup>	GF-677	7 x 6 m	-	2022
4	Alcarràs	283296	4608633	2000	Guara	GF-677	5 x 5 m	-	2022
5	Soses	288321	4601766	2008	Guara	GF-677	5 x 3 m	-	2022

740 <sup>a</sup> Orchards with multiple cultivars, usually in alternating rows.



741 **Table 2.** Models for the cumulative proportion of *Polystigma amygdalinum*

742 airborne ascospores

Model no.	Model <sup>a</sup>	DIC <sup>b</sup>	WAIC <sup>c</sup>	LCPO <sup>d</sup>
1	ADD + ADDwet + ADDvpd + $v$	-3856.11	-3857.62	-1.53
2	ADD + ADDwet + $v$	-3852.24	-3853.60	-1.53
3	ADD + ADDvpd + $v$	-3773.02	-3774.08	-1.50
4	ADD + ADDwet + ADDvpd	-3607.86	-3608.60	-1.43
5	ADD + ADDwet	-3563.35	-3564.24	-1.41
6	ADD + $v$	-3551.87	-3552.87	-1.41
7	ADD + ADDvpd	-3501.95	-3502.55	-1.39
8	ADD	-3466.70	-3467.30	-1.37
9	ADDwet + $v$	-3456.59	-3457.40	-1.37
10	ADDwet + ADDvpd + $v$	-3456.22	-3457.13	-1.37
11	ADDvpd + $v$	-3130.64	-3130.82	-1.24
12	ADDwet + ADDvpd	-3028.19	-3028.82	-1.20
13	ADDwet	-2822.90	-2823.54	-1.12
14	ADDvpd	-2520.92	-2521.19	-1.00
15	$v$	-2289.07	-2289.66	-0.91
16	Null model	-2244.23	-2244.51	-0.89

743 <sup>a</sup>ADD: accumulated degree-days; ADDvpd: ADD considering vapor pressure deficit; ADDwet:

744 ADD considering vapor pressure deficit and rainfall;  $v$ : random effect associated to the year and

745 location. All models include intercept, biofix = 1st January,  $T_{base} = 0^{\circ}C$ .

746 <sup>b</sup>DIC: deviance information criterion.

747 <sup>c</sup>WAIC: widely applicable information criterion.

748 <sup>d</sup>LCPO: logarithmic conditional predictive ordinate.

749 **Table 3.** Mean, standard deviation (SD), quantiles (Q), and mode for the  
 750 parameters and hyperparameters of the selected model for the cumulative  
 751 proportion of *Polystigma amygdalinum* airborne ascospores

<b>Parameters<sup>a</sup></b>	<b>Mean</b>	<b>SD</b>	<b>Q<sub>0.025</sub><sup>c</sup></b>	<b>Q<sub>0.5</sub></b>	<b>Q<sub>0.975</sub><sup>c</sup></b>	<b>Mode</b>
Intercept	-3.213	0.748	-4.756	-3.212	-1.677	-3.207
ADD	0.086	0.004	0.077	0.086	0.094	0.085
ADDwet	1.108	0.064	0.982	1.107	1.235	1.107
<b>Hyperparameters<sup>b</sup></b>						
$\Phi$	3.051	0.136	2.791	3.048	3.325	3.044
$\tau_v$	1.365	1.299	0.130	0.993	4.813	0.372

752 <sup>a</sup> ADD: accumulated degree-days; ADDwet: ADD considering vapor pressure deficit and rainfall.

753 <sup>b</sup>  $\Phi$ : dispersion parameter of the likelihood;  $\tau_v$ : precision of the random effect.

754 <sup>c</sup> 95% credible interval is defined by Q<sub>0.025</sub> and Q<sub>0.975</sub>.

755 **Table 4.** Summary of the posterior distributions of the estimated differences in  
 756 red leaf blotch incidence between the evaluated fungicide programs in 2022 in  
 757 four almond orchards in Lleida region, Spain

Reference level	Fungicide program	Median of estimated differences (95% credible interval)	$P(<0)^a$
UTC	CAL	-0.804 (-0.847, -0.738)	1
	CAL+MET	-0.633 (-0.662, -0.738)	1
	MOD	-0.776 (-0.810, -0.720)	1
	MOD+MET	-0.640 (-0.669, -0.602)	1
CAL	CAL+MET	0.166 (0.110, 0.242)	0
	MOD	0.026 (0.012, 0.049)	0
	MOD+MET	0.160 (0.105, 0.234)	0
CAL+MET	MOD	-0.139 (-0.205, -0.090)	1
	MOD+MET	-0.007 (-0.049, 0.035)	0.625
MOD	MOD+MET	0.133 (0.086, 0.197)	0

758 <sup>a</sup>  $P(<0)$  indicates the probability of the differences being negative.

759 **Table 5.** Relevant dates and number of applications of the fungicide programs  
 760 evaluated for almond red leaf blotch control in 2022 in four almond orchards in  
 761 Lleida region, Spain

Orchard	Open flower <sup>a</sup>	Petal fall <sup>a</sup>	Fungicide program <sup>b</sup>	First application	Last application	Number of applications
2	17 March	22 March	CAL	24 March	25 July	7
			CAL+MET	24 March	31 May	3
			MOD	4 April	7 June	4
			MOD+MET	4 April	31 May	3
3	15 March	22 March	CAL	23 March	29 July	7
			CAL+MET	23 March	21 April	2
			MOD	23 March	5 May	3
			MOD+MET	23 March	21 April	2
4	8 March	15 March	CAL	17 March	20 July	7
			CAL+MET	17 March	21 April	2
			MOD	22 March	26 May	4
			MOD+MET	22 March	21 April	2
5	8 March	15 March	CAL	17 March	20 July	7
			CAL+MET	17 March	21 April	2
			MOD	17 March	19 May	4
			MOD+MET	17 March	21 April	2

762 <sup>a</sup> Phenological stages according to Felipe (1977). Equivalent stages in BBCH scale (Sakar et al.  
 763 2019) were 65 and 67, respectively for each column.

764 <sup>b</sup> A fifth untreated control program (UTC) was included in all orchards.

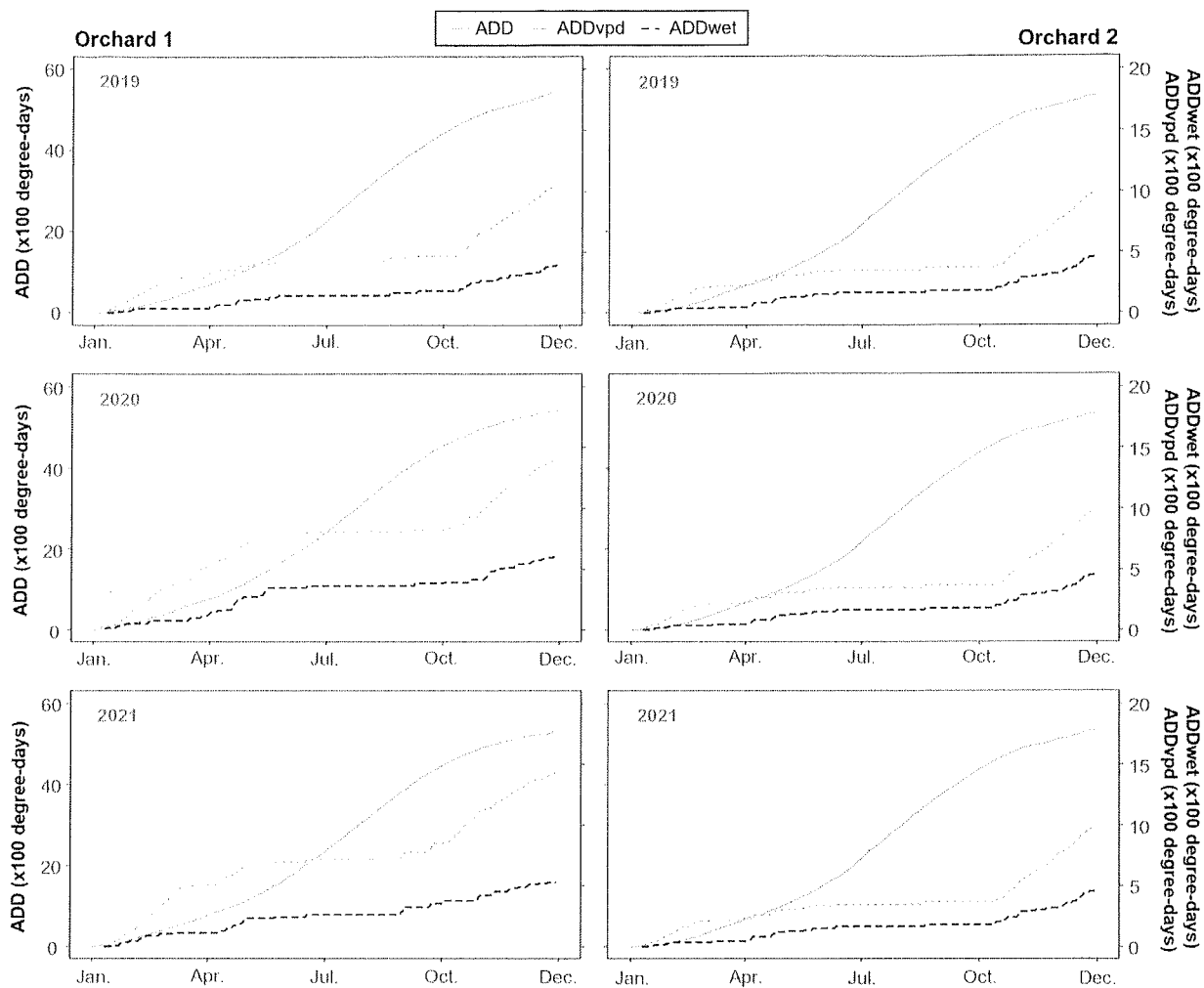
765 **FIGURE LEGENDS**

766 **Fig. 1.** Accumulated degree-days (ADD), ADD considering vapor pressure  
767 deficit (ADDvpd), and ADD considering vapor pressure deficit and rainfall  
768 (ADDwet) in orchards 1 and 2 from 2019 to 2021.

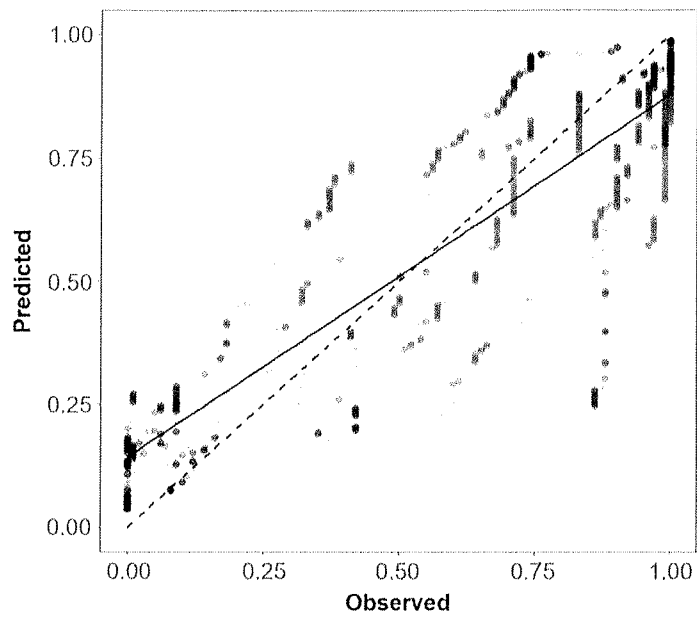
769 **Fig. 2.** Linear regression (solid line) between observed values and the median  
770 of the posterior predictive distribution of the selected model for the cumulative  
771 proportion of *Polystigma amygdalinum* airborne ascospores, including the fixed  
772 effects ADD (accumulated degree-days), ADDwet (ADD considering vapor  
773 pressure deficit and rainfall), and the random effect ( $v$ ) associated to the year  
774 and the location. The dashed line represents the 1:1 relationship.

775 **Fig. 3.** Data (**A**) and median posterior predictive distribution (**B**) for the model of  
776 cumulative proportion of *Polystigma amygdalinum* airborne ascospores, based  
777 on the fixed effects ADD (accumulated degree-days), ADDwet (ADD  
778 considering vapor pressure deficit and rainfall), and the random effect ( $v$ )  
779 associated to the year and the location.

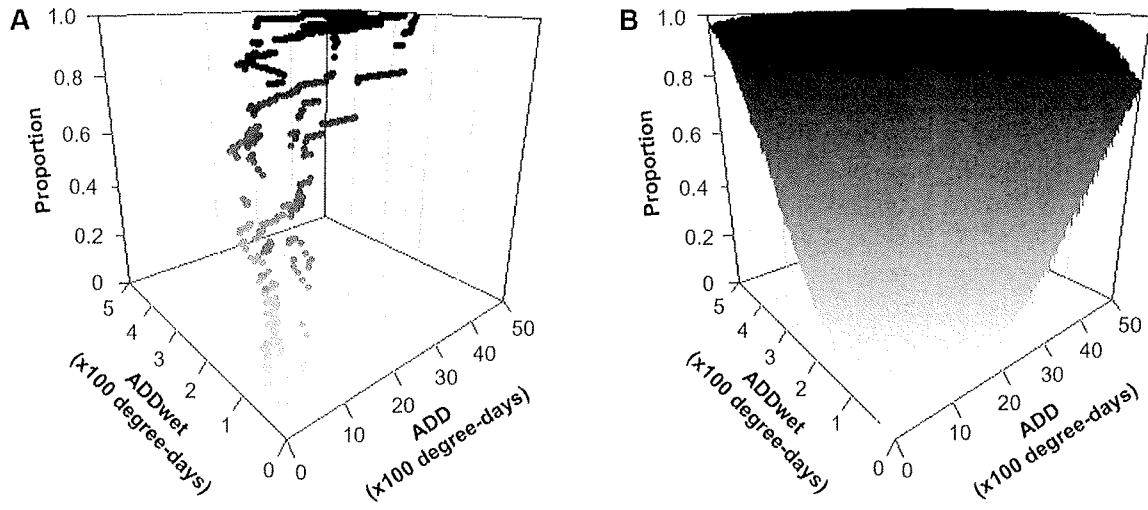
780 **Fig. 4.** Estimated posterior distributions of red leaf blotch incidence for the  
781 fungicide programs evaluated in 2022 in four almond orchards in Lleida region,  
782 Spain. UTC: untreated control; MOD+MET: model-based program +  
783 meteorological criteria; MOD: model-based program; CAL+MET: calendar-  
784 based program + meteorological criteria; CAL: calendar-based program.



787 Fig. 2

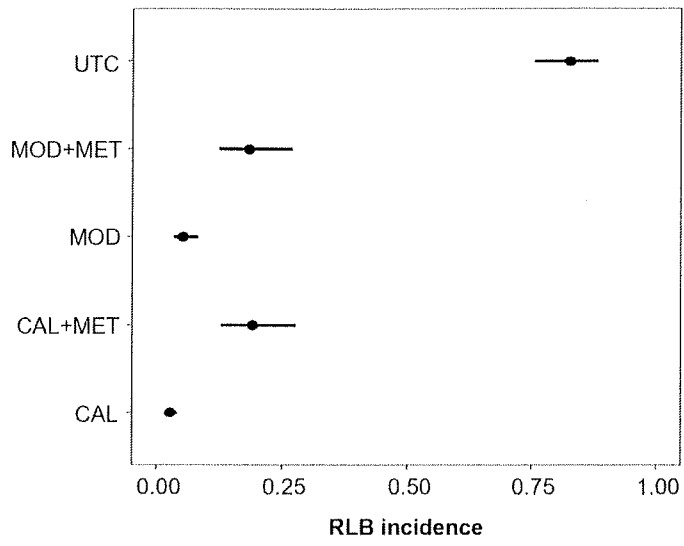


788 Fig. 3





789 **Fig. 4**



791 **Supplementary Table S1. Models for the red leaf blotch incidence**

Model no.	Model <sup>a</sup>	DIC <sup>b</sup>	WAIC <sup>c</sup>	LCPO <sup>d</sup>
1	$\alpha_{0^*} + \text{CAL} + [\text{CAL} + \text{MET}] + \text{MOD} + [\text{MOD} + \text{MET}] + \text{MAR} + u + w$	902.69	938.47	2.94
2	$\alpha_{0^{**}} + \text{CAL} + [\text{CAL} + \text{MET}] + \text{MOD} + [\text{MOD} + \text{MET}] + u + w$	902.71	938.45	2.94
3	$\alpha_{0^{**}} + \text{CAL} + [\text{CAL} + \text{MET}] + \text{MOD} + [\text{MOD} + \text{MET}] + w$	903.44	941.34	2.95
4	$\alpha_{0^*} + \text{CAL} + [\text{CAL} + \text{MET}] + \text{MOD} + [\text{MOD} + \text{MET}] + \text{MAR} + w$	903.46	941.74	2.95
5	$\alpha_{0^*} + \text{CAL} + [\text{CAL} + \text{MET}] + \text{MOD} + [\text{MOD} + \text{MET}] + \text{MAR} + u$	969.91	988.69	3.09
6	$\alpha_{0^{**}} + \text{CAL} + [\text{CAL} + \text{MET}] + \text{MOD} + [\text{MOD} + \text{MET}] + u$	969.91	988.65	3.09
7	$\alpha_{0^*} + \text{CAL} + [\text{CAL} + \text{MET}] + \text{MOD} + [\text{MOD} + \text{MET}] + \text{MAR}$	1363.89	1392.61	4.35
8	$\alpha_{0^{**}} + \text{CAL} + [\text{CAL} + \text{MET}] + \text{MOD} + [\text{MOD} + \text{MET}]$	1375.01	1397.94	4.37
9	$\alpha_{0^{***}} + \text{MAR} + w$	2819.84	17918.60	14.35
10	$\alpha_0 + w$	2838.42	17858.08	14.34
11	$\alpha_{0^{***}} + \text{MAR} + u + w$	3265.09	16264.38	14.20
12	$\alpha_0 + u + w$	3266.29	16260.31	14.20
13	$\alpha_{0^{***}} + \text{MAR} + u$	4246.75	4088.01	13.55
14	$\alpha_0 + u$	4246.75	4088.44	13.55
15	$\alpha_{0^{***}} + \text{MAR} + w$	4475.94	4131.50	14.13
16	$\alpha_0$ (Null model)	4481.85	4078.36	14.08

792 <sup>a</sup>  $\alpha_0$ : intercept;  $\alpha_{0^*}$ : intercept (UTC-GUA);  $\alpha_{0^{**}}$ : intercept (UTC);  $\alpha_{0^{***}}$ : intercept (GUA); CAL:  
793 calendar-based program; [CAL+MET]: calendar-based program + meteorological criteria; MOD:  
794 model-based program; [MOD+MET]: model-based program + meteorological criteria; MAR:  
795 'Marinada' cultivar;  $u$ : random effect associated to the orchard;  $w$ : nested random effect  
796 associated to the block:orchard interaction.  
797 <sup>b</sup> DIC: deviance information criterion.  
798 <sup>c</sup> WAIC: widely applicable information criterion.  
799 <sup>d</sup> LCPO: logarithmic conditional predictive ordinate.

800 **Supplementary Table S2.** Mean, standard deviation (SD), quantiles (Q), and  
 801 mode for the parameters and hyperparameters of the selected model for the red  
 802 leaf blotch incidence

Parameters	Mean	SD	Q <sub>0.025</sub> <sup>b</sup>	Q <sub>0.5</sub>	Q <sub>0.975</sub> <sup>b</sup>	Mode
B <sub>0</sub> +(UTC)	1.569	0.228	1.120	1.568	2.023	1.567
CAL	-5.294	0.165	-5.619	-5.294	-4.970	-5.294
CAL+MET	-3.016	0.098	-3.207	-3.016	-2.825	-3.016
MOD	-4.507	0.129	-4.760	-4.507	-4.253	-4.507
MOD+MET	-3.060	0.098	-3.253	-3.060	-2.868	-3.060
<b>Hyperparameters<sup>a</sup></b>						
$\tau_w$	1.490	0.568	0.607	1.415	2.808	1.266

803 <sup>a</sup>  $\tau_w$ : precision of the nested random effect block:orchard.

804 <sup>b</sup> 95% credible interval is defined by Q<sub>0.025</sub> and Q<sub>0.975</sub>.